Global Journal of Researches in Engineering: F
Electrical and Electronics Engineering
Volume 20 Issue 4 Version 1.0 Year 2020
Type: Double Blind Peer Reviewed International Research Journal
Publisher: Global Journals
Online ISSN: 2249-4596 & Print ISSN: 0975-5861

Detection and Parameter Extraction of Low Probability of Intercept Frequency Hopping Signals using the Spectrogram and the Reassigned Spectrogram

By Daniel L. Stevens

Abstract- Low probability of intercept radar signals, which are often problematic to detect and characterize, have as their goal 'to see and not be seen'. Digital intercept receivers are currently moving away from Fourier-based analysis and towards classical time-frequency analysis techniques for the purpose of analyzing these low probability of intercept radar signals. Although these classical time-frequency analysis techniques are an improvement over existing Fourier-based techniques, they still suffer from a lack of readability –which can be caused by poor time-frequency localization (such as the spectrogram), which may in turn lead to inaccurate detection and parameter extraction. In this study, the reassignment method, because of its ability to improve time-frequency localization, is proposed as an improved signal analysis technique to address the poor time-frequency localization deficiency of the spectrogram. This paper presents the novel approach of characterizing low probability of intercept frequency hopping radar signals through utilization and direct comparison of the spectrogram versus the reassigned spectrogram.

GJRE-F Classification: *FOR Code: 090609*

Strictly as per the compliance and regulations of:

Detection and Parameter Extraction of Low Probability of Intercept Frequency Hopping Signals using the Spectrogram and the Reassigned Spectrogram[1]

Daniel L. Stevens

Abstract- Low probability of intercept radar signals, which are often problematic to detect and characterize, have as their goal 'to see and not be seen'. Digital intercept receivers are currently moving away from Fourier-based analysis and towards classical time-frequency analysis techniques for the purpose of analyzing these low probability of intercept radar signals. Although these classical time-frequency analysis techniques are an improvement over existing Fourier-based techniques, they still suffer from a lack of readability –which can be caused by poor time-frequency localization (such as the spectrogram), which may in turn lead to inaccurate detection and parameter extraction. In this study, the reassignment method, because of its ability to improve time-frequency localization, is proposed as an improved signal analysis technique to address the poor time-frequency localization deficiency of the spectrogram. This paper presents the novel approach of characterizing low probability of intercept frequency hopping radar signals through utilization and direct comparison of the spectrogram versus the reassigned spectrogram. A 4 component frequency hopping low probability of intercept radar signal was analyzed. The following metrics were used for evaluation: average percent error of: carrier frequency, modulation bandwidth, modulation period, and time-frequency localization. Also used were averages: percent detection, lowest signal-to-noise ratio for signal detection, and plot (processing) time. Experimental results demonstrate that the 'squeezing' quality of the reassignment method produced an improved readability over the classical time-frequency analysis technique and consequently, the reassigned spectrogram produced more accurate characterization metrics than the spectrogram. An improvement in performance may well translate into saved equipment and lives.

I. Introduction

a) *Frequency hopping techniques*

A low probability of intercept (LPI) radar that uses frequency hopping techniques changes the transmitting frequency in time over a wide bandwidth in order to prevent an intercept receiver from intercepting the waveform. The frequency slots used are chosen from a frequency hopping sequence, and it is this unknown sequence that gives the radar the advantage over the intercept receiver in terms of processing gain. The frequency sequence appears random to the intercept receiver, and so the possibility of it following the changes in frequency is remote [PAC09]. This prevents a jammer from reactively jamming the transmitted frequency [ADA04]. Frequency hopping radar performance depends only slightly on the code used, given that certain properties are met. This allows for a larger variety of codes, making it more difficult to intercept[1].

b) *Time-frequency signal analysis*

Time-frequency signal analysis involves the analysis and processing of signals with time-varying frequency content. Such signals are best represented by a time-frequency distribution [PAP95], [HAN00], which is intended to show how the energy of the signal is distributed over the two-dimensional time-frequency plane [WEI03], [LIX08], [OZD03]. Processing of the signal may then exploit the features produced by the concentration of signal energy in two dimensions (time and frequency), instead of only one dimension (time or frequency) [BOA03], [LIY03]. Since noise tends to spread out evenly over the time-frequency domain, while signals concentrate their energies within limited time intervals and frequency bands; the local SNR of a noisy signal can be improved simply by using time-frequency analysis [XIA99]. Also, the intercept receiver can increase its processing gain by implementing time-frequency signal analysis [GUL08]. In addition, time-frequency distributions are useful for the visual interpretation of signal dynamics [RAN01]. An experienced operator can quickly detect a signal and extract the signal parameters by analyzing the time-frequency distribution [ANJ09].

Some of the more common classical time-frequency analysis techniques include the Wigner-Ville distribution (WVD), Choi-Williams distribution (CWD), spectrogram and scalogram. The WVD exhibits the highest signal energy concentration [PAC09], but has the worst cross-term interference, which can severely limit the readability of a time-frequency representation

Author: *Air Force Research Laboratory, Rome, NY.*
e-mail: daniel.stevens.7@us.af.mil

[1] Approved for Public Release; Distribution Unlimited: Case Number 88ABW-2020-2109

[GUL08], [BOA03]. The CWD is a member of Cohen's class, which adds a smoothing kernel to help reduce cross-term interference [BOA03]. The CWD, as with all members of Cohen's class, is faced with a trade-off between cross-term reduction and time-frequency localization. The spectrogram is the magnitude squared of the short-time Fourier transform (STFT) [HLA92], [MIT01]. It has poorer time-frequency localization but less cross-term interference than either the WVD or CWD, and its cross-terms are limited to regions where the signals overlap [BOA03]. The scalogram is the magnitude squared of the wavelet transform and can be used as a time-frequency distribution [COH02], [GAL05]. Like the spectrogram, the scalogram has cross-terms that are limited to regions where the signals overlap [BOA03], [HLA92].

Though classical time-frequency analysis techniques are a great improvement over Fourier analysis techniques, they may suffer from poor time-frequency localization, as described above. This may result in degraded readability of time-frequency representations, potentially leading to inaccurate LPI radar signal detection and parameter extraction metrics, and as such, can lead to decisions based on inaccurate information.

c) Reassignment method

A promising avenue for overcoming this deficiency is the utilization of the reassignment method. The reassignment method, which can be applied to most energy distributions [HIP00], has, in theory, a perfectly localized distribution for chirps, tones and impulses [BOA03], making it a good candidate for the analysis of certain LPI radar signals, such as the triangular modulated frequency modulated continuous wave (FMCW) (which can be viewed as back-to-back chirps) and the frequency shift keying (FSK) (which can be viewed as tones).

d) Spectrogram and reassigned spectrogram

The spectrogram is defined as the magnitude squared of the STFT [BOA03], [HIP00], [HLA92], [MIT01], [PAC09]. For non-stationary signals, the STFT is usually in the form of the spectrogram [GRI08].

The STFT of a signal $x(u)$is given in equation 2.5 as:

$$F_x(t,f;h) = \int_{-\infty}^{+\infty} x(u)h\,(ut)e^{-j\,2\pi fu}\,du \qquad (2.5)$$

Where $h(t)$ is a short time analysis window localized around $t = 0$ and $f = 0$. Because multiplication by the relatively short window $h(u-t)$ effectively suppresses the signal outside a neighborhood around the analysis point $u = t$, the STFT is a 'local' spectrum of the signal $x(u)$ around t. Think of the window $h(t)$ as sliding along the signal $x(u)$ and for each shift $h(u-t)$ we compute the usual Fourier transform of the product function $x(u)h(u-t)$. The observation window allows localization of the spectrum in time, but also smears the spectrum in frequency in accordance with the uncertainty principle, leading to a trade-off between time resolution and frequency resolution. In general, if the window is short, the time resolution is good, but the frequency resolution is poor, and if the window is long, the frequency resolution is good, but the time resolution is poor.

The STFT was the first tool devised for analyzing a signal in both time and frequency simultaneously. For analysis of human speech, the main method was, and still is, the STFT. In general, the STFT is still the most widely used method for studying non-stationary signals [COH95].

The spectrogram (the squared modulus of the STFT) is given by equation 2.6 as:

$$S_x(t,f) = \left|\int_{-\infty}^{+\infty} x(u)\,h(u-t)e^{-j\,2\pi fu}\,du\right|^2 \qquad (2.6)$$

The spectrogram is a real-valued and non-negative distribution. Since the window h of the STFT is assumed of unit energy, the spectrogram satisfies the global energy distribution property. Thus we can interpret the spectrogram as a measure of the energy of the signal contained in the time-frequency domain centered on the point (t, f) and whose shape is independent of this localization.

Here are some properties of the spectrogram: 1) time and frequency covariance - the spectrogram preserves time and frequency shifts, thus the spectrogram is an element of the class of quadratic time-frequency distributions that are covariant by translation in time and in frequency (i.e. Cohen's class); 2) time-frequency resolution - the time-frequency resolution of the spectrogram is limited exactly as it is for the STFT; there is a trade-off between time resolution and frequency resolution. This poor resolution is the main drawback of this representation; 3) interference structure - as it is a quadratic (or bilinear) representation, the spectrogram of the sum of two signals is not the sum of the two spectrograms (quadratic superposition principle); there is a cross-spectrogram part and a real part. Thus, as for every quadratic distribution, the spectrogram presents interference terms; however, those interference terms are restricted to those regions of the time-frequency plane where the signals overlap. Thus if the signal components are sufficiently distant so that their spectrograms do not overlap significantly, then the interference term will nearly be identically zero [COH95], [HLA92], [ISI96].

The original idea of reassignment was introduced in an attempt to improve the spectrogram [OZD03]. As with any other bilinear energy distribution, the spectrogram is faced with an unavoidable trade-off between the reduction of misleading interference terms and a sharp localization of the signal components.

We can define the spectrogram as a two-dimensional convolution of the WVD of the signal by the WVD of the analysis window, as in equation 2.9:

$$S_x(t,f;h) = \iint_{-\infty}^{+\infty} W_x(s,\xi) W_h(t-s, f-\xi)\, ds\, d\xi \quad (2.9)$$

Therefore, the distribution reduces the interference terms of the signal's WVD, but at the expense of time and frequency localization. However, a closer look at equation 2.9 shows that $W_h(t-s, f-\xi)$ delimits a time-frequency domain at the vicinity of the (t,f) point, inside which a weighted average of the signal's WVD values is performed. The key point of the reassignment principle is that these values have no reason to be symmetrically distributed around (t,f), which is the geometrical center of this domain. Therefore, their average should not be assigned at this point, but rather at the center of gravity of this domain, which is much more representative of the local energy distribution of the signal [BOA03]. Reasoning with a mechanical analogy, the local energy distribution $W_h(t-s, f-\xi)W_x(s,\xi)$ (as a function of s and ξ) can be considered as a mass distribution, and it is much more accurate to assign the total mass (i.e. the spectrogram value) to the center of gravity of the domain rather than to its geometrical center. Another way to look at it is this: the total mass of an object is assigned to its geometrical center, an arbitrary point which except in the very specific case of a homogeneous distribution, has no reason to suit the actual distribution. A much more meaningful choice is to assign the total mass of an object, as well as the spectrogram value, to the center of gravity of their respective distribution [BOA03].

This is exactly how the reassignment method proceeds: it moves each value of the spectrogram computed at any point (t,f) to another point $(\hat{t},\hat{f})$ which is the center of gravity of the signal energy distribution around (t,f) (see equations 2.10 and 2.11) [LIX08]:

$$\hat{t}(x;t,f) = \frac{\iint_{-\infty}^{+\infty} s\, W_h(t-s,f-\xi) W_x(s,\xi)\, ds\, d\xi}{\iint_{-\infty}^{+\infty} W_h(t-s,f-\xi) W_x(s,\xi)\, ds\, d\xi} \quad (2.10)$$

$$\hat{f}(x;t,f) = \frac{\iint_{-\infty}^{+\infty} \xi\, W_h(t-s,f-\xi) W_x(s,\xi)\, ds\, d\xi}{\iint_{-\infty}^{+\infty} W_h(t-s,f-\xi) W_x(s,\xi)\, ds\, d\xi} \quad (2.11)$$

and thus leads to a reassigned spectrogram (equation (2.12)), whose value at any point (t',f') is the sum of all the spectrogram values reassigned to this point:

$$S_x^{(r)}(t',f';h) = \iint_{-\infty}^{+\infty} S_x(t,f;h)\,\delta\big(t' - \hat{t}(x;t,f)\big)\,\delta\big(f' - \hat{f}(x;t,f)\big)\, dt\, df \quad (2.12)$$

One of the most interesting properties of this new distribution is that it also uses the phase information of the STFT, and not only its squared modulus as in the spectrogram. It uses this information from the phase spectrum to sharpen the amplitude estimates in time and frequency. This can be seen from the following expressions of the reassignment operators:

$$\hat{t}(x;t,f) = -\frac{d\Phi_x(t,f;h)}{df} \quad (2.13)$$

$$\hat{f}(x;t,f) = f + \frac{d\Phi_x(t,f;h)}{dt} \quad (2.14)$$

where $\Phi_x(t,f;h)$ is the phase of the STFT of x : $\Phi_x(t,f;h) = \arg\,(F_x$ (t, f; h)). However, these expressions (equations 2.13 and 2.14) do not lead to an efficient implementation, and have to be replaced by equations 2.15 (local group delay) and 2.16 (local instantaneous frequency):

$$\hat{t}(x;t,f) = t - \Re\left\{\frac{F_x(t,f;T_h)F_x^*(t,f;h)}{\left|F_{x(t,f;h)}\right|^2}\right\} \quad (2.15)$$

$$\hat{f}(x;t,f) = f - \Im\left\{\frac{F_x(t,f;D_h)F_x^*(t,f;h)}{\left|F_{x(t,f;h)}\right|^2}\right\} \quad (2.16)$$

where $T_h(t) = t \times h(t)$ and $D_h(t) = \frac{dh}{dt}(t)$. This leads to an efficient implementation for the reassigned spectrogram without explicitly computing the partial derivatives of phase. The reassigned spectrogram may thus be computed by using 3 STFTs, each having a different window (the window function h; the same window with a weighted time ramp t*h; the derivative of the window function h with respect to time (dh/dt)). Reassigned spectrograms are therefore very easy to implement, and do not require a drastic increase in computational complexity.

One of the most important properties of the reassignment method is that the application of the reassignment process to any distribution of Cohen's class theoretically yields perfectly localized distributions for chirp signals, frequency tones, and impulses, since the WVD does so also. As mentioned earlier, this is one of the reasons that the reassignment method can be chosen as a signal process analysis tool for analyzing LPI radar waveforms such as triangular modulated FMCW waveforms (which can be viewed as back-to-back chirps) and FSK waveforms (which can be viewed as frequency tones).

The reassignment method provides readability improvement. The components are much better localized and very concentrated. In order to rectify the classical time-frequency analysis deficiency of poor time-frequency localization, there needs to be a method that produces more concentrated distributions, which the reassignment method does. This squeezing quality of the reassignment method lead to improved readability - which leads to more accurate metrics extracted – which in turn, creates a more informed and safer intercept receiver environment.

II. Methodology

The methodologies detailed in this section describe the processes involved in obtaining and comparing metrics between the classical time-frequency analysis technique of the spectrogram vs. the reassigned spectrogram, for the detection and characterization of low probability of intercept frequency hopping radar signals.

The tools used for this testing were: MATLAB (version 8.3), Signal Processing Toolbox (version 6.21), Wavelet Toolbox (version 4.13), Image Processing Toolbox (version 9.0), Time-Frequency Toolbox (version 1.0) (http://tftb.nongnu.org/).

All testing was accomplished on a desktop computer (Dell Precision T1700; Processor - Intel Xeon CPU E3-1226 v3 3.30GHz; Installed RAM - 32.0GB; System type - 64-bit operating system, x64-based processor).

Testing was performed for the 4 component frequency hopping waveform, whose parameters were chosen for academic validation of signal processing techniques. Due to computer processing resources they were not meant to represent real-world values. The number of samples for each test was chosen to be 512, which seemed to be the optimum size for the desktop computer. Testing was performed at three different SNR levels: 10dB, 0dB, and the lowest SNR at which the signal could be detected. The noise added was white Gaussian noise, which best reflects the thermal noise present in the IF section of an intercept receiver [PAC09]. Kaiser windowing was used, when windowing was applicable. 100 runs were performed for each test, for statistical purposes. The plots included in this paper were done at a threshold of 5% of the maximum intensity and were linear scale (not dB) of analytic (complex) signals; the color bar represented intensity. The signal processing tools used for each task were the spectrogram and the reassigned spectrogram.

The 4 component frequency hopping signal (prevalent in the LPI arena [AMS09]) had the following parameters: sampling frequency=5KHz; carrier frequencies=1KHz, 1.75KHz, 0.75KHz, 1.25KHz; modulation bandwidth=1KHz; modulation period=.025sec.

After each particular run of each test, metrics were extracted from the time-frequency representation. The different metrics extracted were as follows:

Plot (processing) time: Time required for plot to be displayed.

Percent detection: Percent of time signal was detected - signal was declared a detection if any portion of each of the signal components (4 signal components for frequency hopping) exceeded a set threshold (a certain percentage of the maximum intensity of the time-frequency representation).

Threshold percentages were determined based on visual detections of low SNR signals (lowest SNR at which the signal could be visually detected in the time-frequency representation) (see Figure 1).

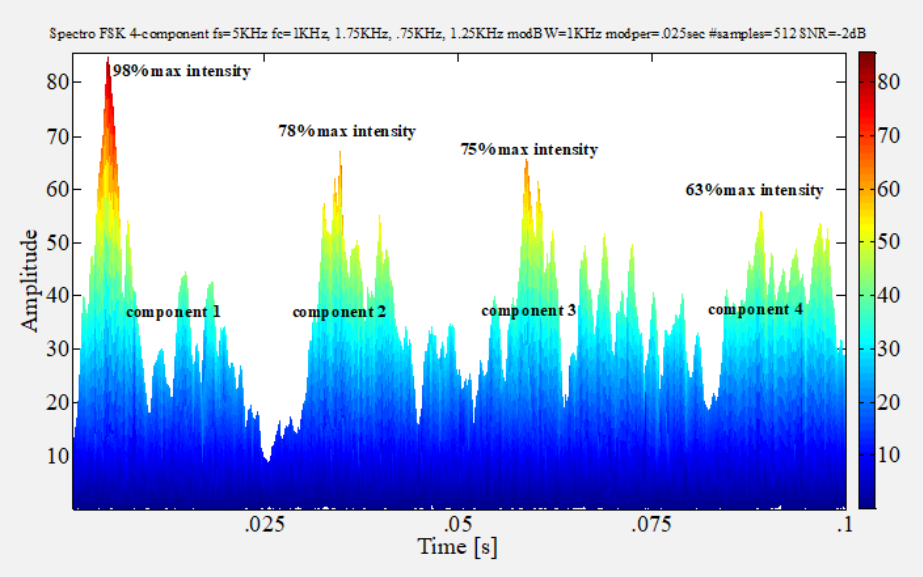

Figure 1: Threshold percentage determination. This plot is an amplitude vs. time (x-z view) of the spectrogram of a frequency hopping 4 component signal (512 samples, SNR= -2dB). For visually detected low SNR plots (like this one), the percent of max intensity for the peak z-value of each of the signal components was noted (here 98%, 78%, 75%, 63%), and the lowest of these 4 values was recorded (63%). Ten test runs were performed for both time-frequency analysis tools (spectrogram and reassigned spectrogram) for this waveform. The average of these recorded low values was determined and then assigned as the threshold for that particular time-frequency analysis tool. Note - the threshold value assigned for the spectrogram was 60%.

Thresholds were assigned as follows: spectrogram (60%); reassigned spectrogram (50%).

For percent detection determination, these threshold values were included in the time-frequency plot algorithms so that the thresholds could be applied automatically during the plotting process. From the threshold plot, the signal was declared a detection if any portion of each of the signal components was visible (see Figure 2).

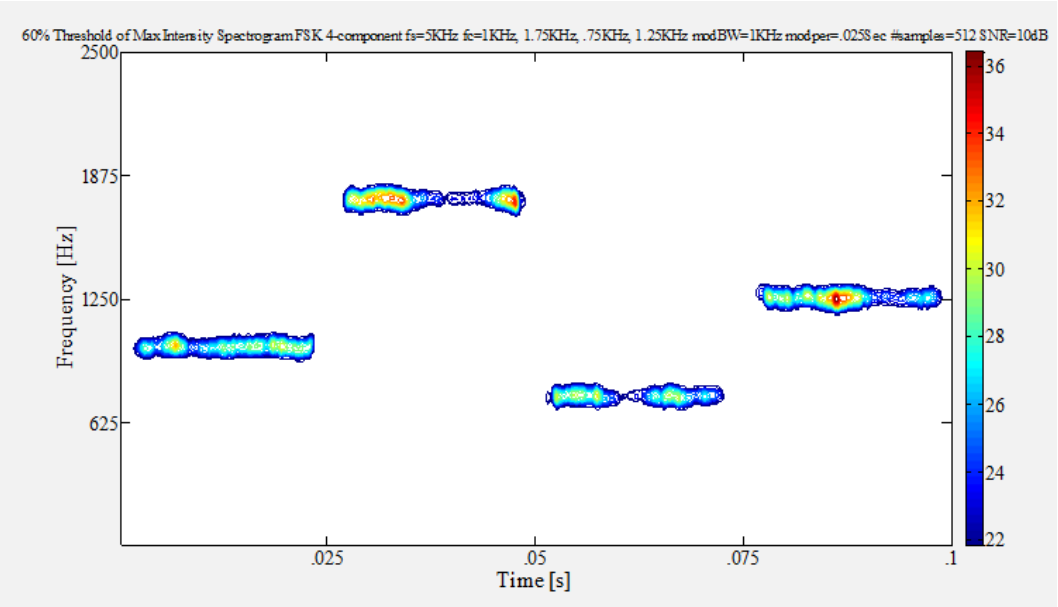

Figure 2: Percent detection (time-frequency). This plot is a time vs. frequency (x-y view) of the spectrogram of a 4 component frequency hopping signal (512 samples, SNR=10dB) with threshold value automatically set to 60%. From this threshold plot, the signal was declared a (visual) detection because at least a portion of each of the 4 FSK signal components was visible.

Carrier frequency: The frequency corresponding to the maximum intensity of the time-frequency representation (there are multiple carrier frequencies (4 ea) for the 4 component frequency hopping waveform) (see Figure 3).

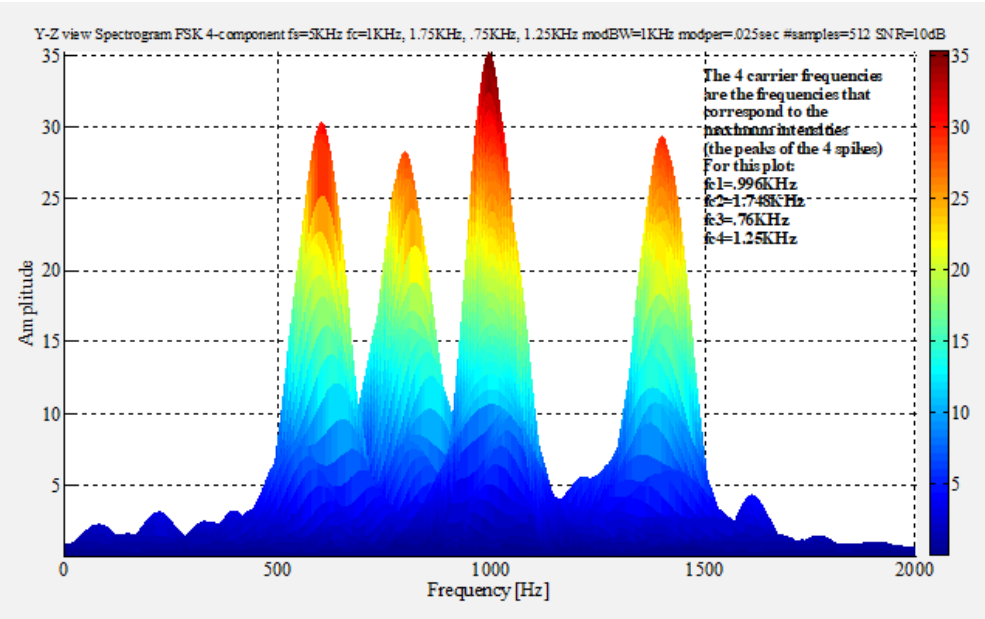

Figure 3: Determination of carrier frequency. Spectrogram of a 4 component frequency hopping signal (512 samples, SNR=10dB). From the frequency-intensity (y-z) view, the 4 maximum intensity values (1 for each carrier frequency) are manually determined. The frequencies corresponding to those 4 max intensity values are the 4 carrier frequencies (for this plot fc1=996 Hz, fc2=1748Hz, fc3=760Hz, fc4=1250Hz).

Modulation bandwidth: Distance from highest frequency value of signal (at a threshold of 20% maximum intensity) to lowest frequency value of signal (at same threshold) in Y-direction (frequency).

The threshold percentage was determined based on manual measurement of the modulation bandwidth of the signal in the time-frequency representation. This was accomplished for ten test runs of each time-frequency analysis tool (spectrogram and reassigned spectrogram), for the 4 component frequency hopping waveform. During each manual measurement, the max intensity of the high and low measuring points was recorded. The average of the max intensity values for these test runs was 20%. This was adopted as the threshold value, and is representative of what is obtained when performing manual measurements. This 20% threshold was also implemented for determining the modulation period and the time-frequency localization (both are described below).

For modulation bandwidth determination, the 20% threshold value was included in the time-frequency plot algorithms so that the threshold could be applied automatically during the plotting process. From the threshold plot, the modulation bandwidth was manually measured (see Figure 4).

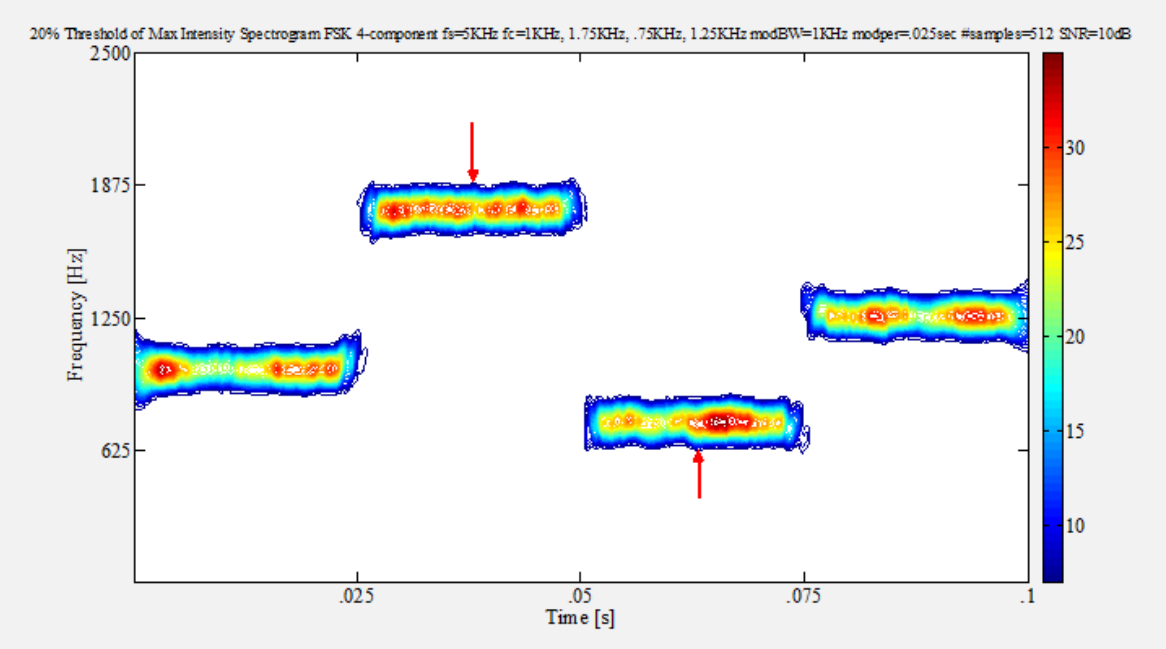

Figure 4: Modulation bandwidth determination. This plot is a time vs. frequency (x-y view) of the spectrogram of a 4 component frequency hopping signal (512 samples, SNR=10dB) with threshold value automatically set to 20%. From this threshold plot, the modulation bandwidth was measured manually from the highest frequency value of the signal (top red arrow) to the lowest frequency value of the signal (bottom red arrow) in the y-direction (frequency).

Modulation period: From Figure 5 (which is at a threshold of 20% maximum intensity), the modulation period is the manual measurement of the width of each of the 4 frequency hopping signals in the x-direction (time), and then the average of the 4 signals is calculated.

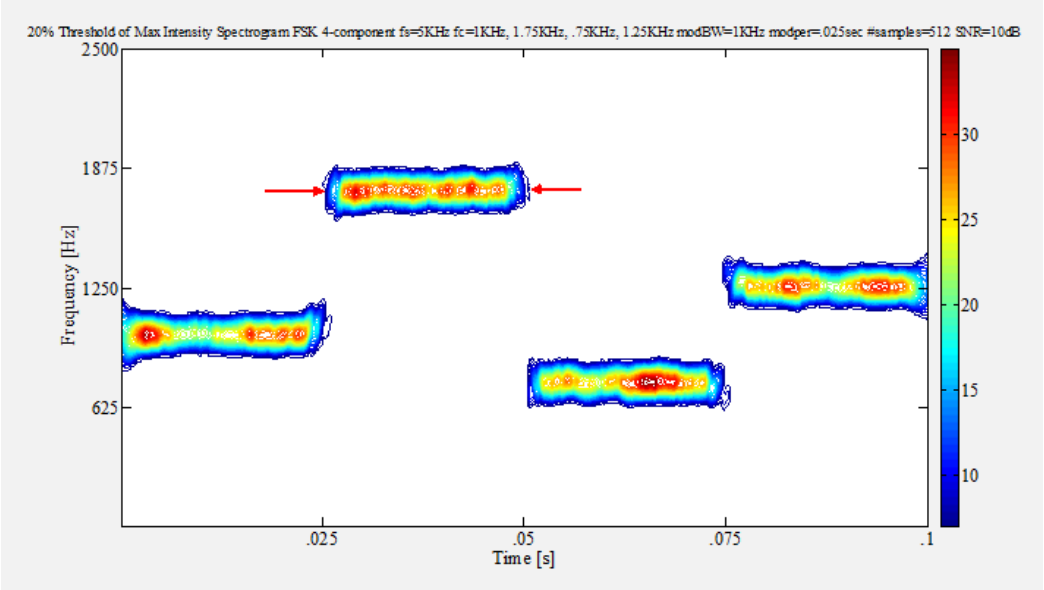

Figure 5: Modulation period determination. This plot is a time vs. frequency (x-y view) of the spectrogram of a 4 component frequency hopping signal (512 samples, SNR=10dB) with threshold value automatically set to 20%. From this threshold plot, the modulation period was measured manually from the left side of the signal (left red arrow) to the right side of the signal (right red arrow) in the x-direction (time). This was done for all 4 signal components, and the average value was determined.

Time-frequency localization: From Figure 6, the time-frequency localization is a manual measurement (at a threshold of 20% maximum intensity) of the 'thickness' (in the y-direction) of the center of each of the 4 frequency hopping signal components, and then the average of the 4 values are determined. The average frequency 'thickness' is then converted to: percent of the entire y-axis.

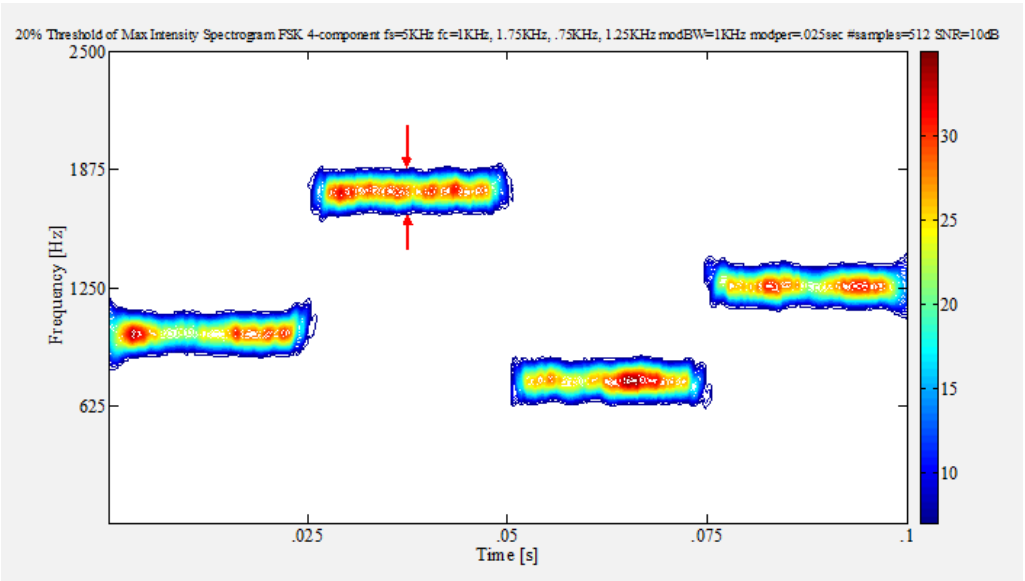

Figure 6: Time-frequency localization determination. This plot is a time vs. frequency (x-y view) for the spectrogram of a 4 component frequency hopping signal (512 samples, SNR=10dB) with threshold value automatically set to 20%. From this threshold plot, the time-frequency localization was measured manually from the top of the signal (top red arrow) to the bottom of the signal (bottom red arrow) in the y-direction (frequency). This frequency 'thickness' value was then converted to: % of entire y-axis.

Lowest detectable SNR: The lowest SNR level at which at least a portion of each of the signal components exceeded the set threshold listed in the percent detection section above.

For lowest detectable SNR determination, these threshold values were included in the time-frequency plot algorithms so that the thresholds could be applied automatically during the plotting process. From the

threshold plot, the signal was declared a detection if any portion of each of the signal components was visible. The lowest SNR level for which the signal was declared a detection is the lowest detectable SNR (see Figure 7).

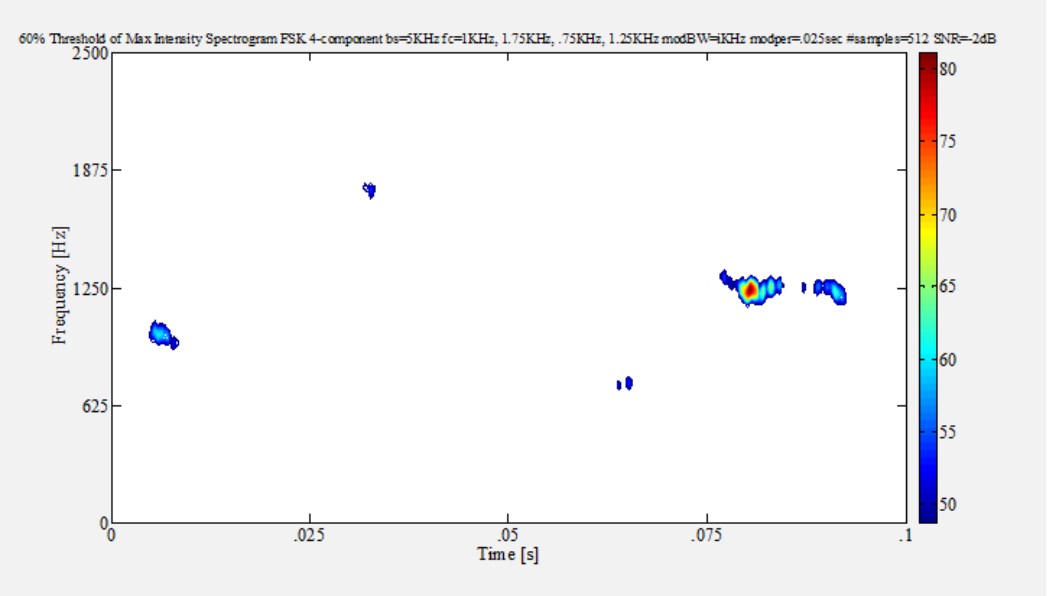

Figure 7: Lowest detectable SNR. This plot is a time vs. frequency (x-y view) of the spectrogram of a 4 component frequency hopping signal (512 samples, SNR=-2dB) with threshold value automatically set to 60%. From this threshold plot, the signal was declared a (visual) detection because at least a portion of each of the 4 frequency hopping signal components was visible. Note that the average lowest detectable SNR for the spectrogram was determined to be -2.7dB. Compare to Figure 2, which is the same plot, except that it has an SNR level equal to 10dB.

The data from all 100 runs for each test was used to produce the actual, error, and percent error for each of these metrics listed above.

The metrics from the spectrogram were then compared to the metrics from the reassigned spectrogram. By and large, the reassigned spectrogram outperformed the spectrogram, as will be shown in the results section.

III. Results

Table 1 presents the overall test metrics for the signal processing analysis techniques used in this testing (spectrogram versusre assigned spectrogram).

Table 1: Overall test metrics (average percent error: carrier frequency, modulation bandwidth, modulation period, time-frequency localization-y; average: percent detection, lowest detectable snr, plot time) for spectrogram versusreassigned spectrogram.

Parameters	Spectrogram	Reassigned spectrogram
carrier frequency	0.93%	0.74%
modulation bandwidth	25.70%	10.82%
modulation period	11.84%	9.30%
time-frequency localization-y	9.09%	4.05%
percent detection	67.24%	86.84%
lowest detectable snr	-2.7db	-3.5db
plottime	4.72s	7.62s

From Table 1, the reassigned spectrogram outperformed the spectrogram in average percent error: carrier frequency (0.74% vs. 0.93%), modulation bandwidth (10.82% vs. 25.70%), modulation period (9.30% vs. 11.84%), and time-frequency localization (y-direction) (4.05% vs. 9.09%);and in average: percent detection (86.84% vs. 67.24%), and lowest detectable SNR (-3.5db vs. -2.7db), while the spectrogram outperformed the reassigned spectrogram in average plot time (4.72s vs. 7.62s).

Figure 8 shows comparative plots of the spectrogram vs. the reassigned spectrogram (4 component frequency hopping) at SNRs of 10dB (top), 0dB (middle), and -3dB (bottom).

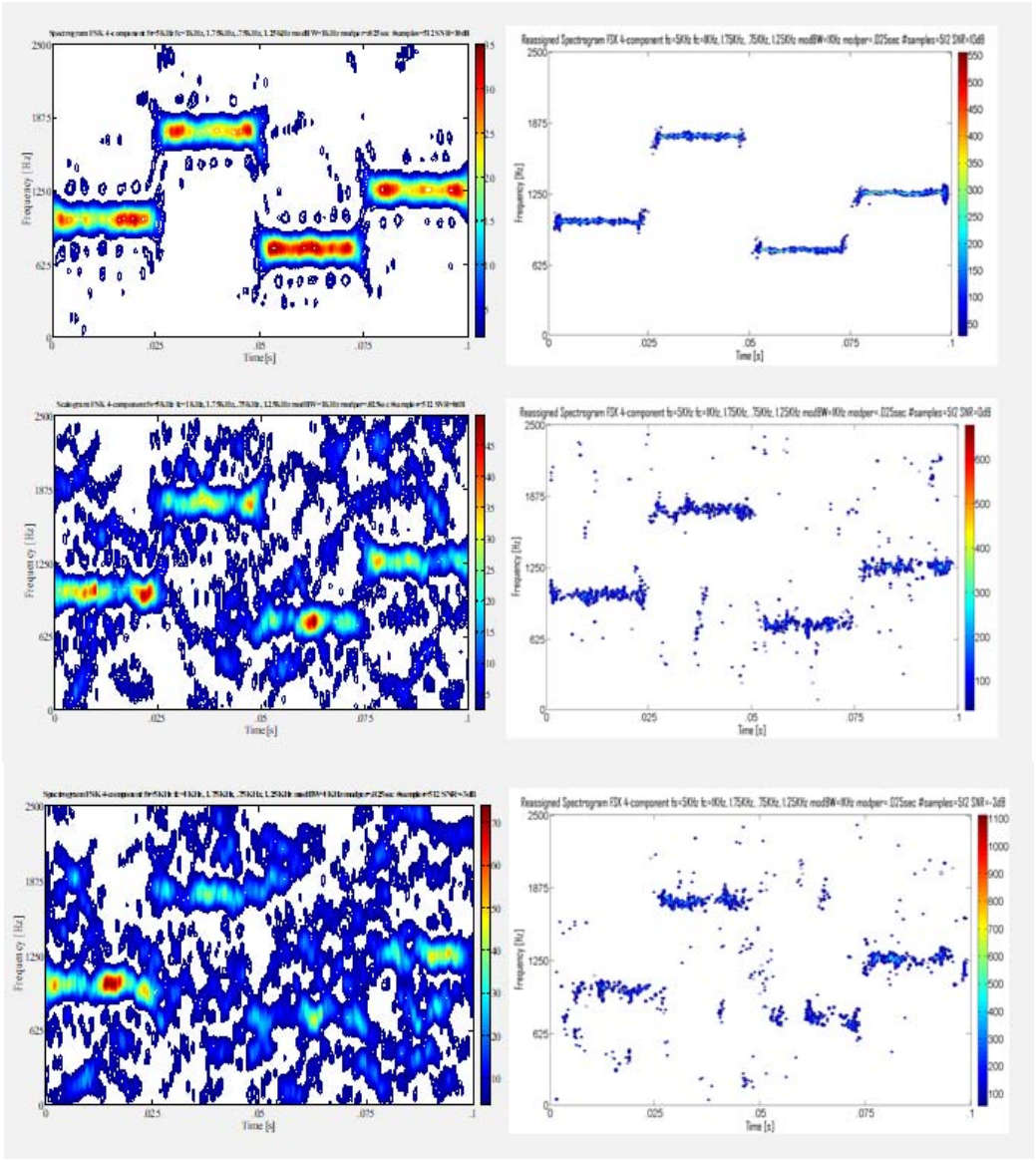

Figure 8: Comparative plots of the 4 component frequency hopping low probability of intercept radar signals (spectrogram (left-hand side) vs. the reassigned spectrogram (right-hand side)). The SNR for the top row is 10dB, for the middle row is 0dB, and for the bottom row is -3dB. In general, the reassigned spectrogram signals appear more localized ('thinner') than do the spectrogram signals. In addition, the reassigned spectrogram signals appear more readable than the spectrogram signals at every SNR level.

IV. Discussion

This section will elaborate on the results from the previous section.

From Table 1, the performance of the spectrogram and the reassigned spectrogram will be summarized, including strengths, weaknesses, and generic scenarios in which each particular signal analysis tool might be used.

The spectrogram outperformed the reassigned spectrogram in average plot time (4.72s vs 7.62s). However, the spectrogram was outperformed by the reassigned spectrogram in every other category. The spectrogram's extreme reduction of cross-term interference is grounds for its good plot time, but at the expense of signal localization (i.e. it produces a 'thicker' signal (as is seen in Figure 8) – due to the trade-off between cross-term interference and signal localization). This poor signal localization ('thicker' signal), coupled with the reassigned spectrogram's 'squeezing' quality, can account for the spectrogram being outperformed by the reassigned spectrogram in the areas of: average percent error of modulation bandwidth, modulation period, time-frequency localization (y-direction), lowest detectable SNR, and percent detection. Note that average percent detection and lowest detectable SNR are both based on visual detection in the time-frequency representation. Figure 8 clearly shows that the signals in the reassigned spectrogram plots are more readable

than those in the spectrogram plots, which accounts for the reassigned spectrogram's better average percent detection and lowest detectable SNR. The spectrogram might be used in a scenario where a short plot time is necessary, but where accurate parameters are not as vital. Such a scenario might be a 'quick and dirty' check to see if a signal is present, without accurate extraction of its parameters. The reassigned spectrogram might be used in a scenario where you need accurate parameters, in a low SNR environment, in a quick time frame.

V. Conclusions

Digital intercept receivers, whose main job is to detect and extract parameters from low probability of intercept radar signals, are currently moving away from Fourier-based analysis and towards classical time-frequency analysis techniques, such as the spectrogram, for the purpose of analyzing low probability of intercept radar signals. Based on the research performed for this paper (the novel direct comparison of the spectrogram versus the reassigned spectrogram for the signal analysis of low probability of intercept frequency hopping radar signals) it was shown that the reassigned spectrogram by-and-large outperformed the spectrogram in analyzing these low probability of intercept radar signals - for reasons brought out in the discussion section above. More accurate characterization metrics could well translate into saved equipment and lives.

Future plans include analysis of additional low probability of intercept radar waveforms, using additional time-frequency analysis and reassignment method techniques.

References Références Referencias

1. [HLA92] Hlawatsch, F., Boudreaux-Bartels, G.F., Linear and Quadratic Time-Frequency Signal Representations. IEEE Signal Processing Mag., Vol. 9, No. 2, pp. 21-67, April 1992.
2. [ISI96] Auger, F., Flandrin, P., Goncalves, P., Lemoine, O., Time-Frequency Toolbox Users Manual. Centre National de la Recherche Scientifique and Rice University, 1996.
3. [LIX08] Li, X., Bi, G., A New Reassigned Time-Frequency Representation. 16th European Signal Processing Conference, Lausanne, Switzerland, pp. 1-4, August 25-29, 2008.
4. [LIY03] Li, Y., Xiao, X., Recursive Filtering Radon-Ambiguity Transform Algorithm for Detecting Multi-LFM Signals. Journal of Electronics (China), Vol. 20, No. 3, pp. 161-166, May 2003.
5. [MIT01] Mitra, S., Digital Signal Processing, A Computer-Based Approach, Second Edition. McGraw-Hill, Boston, MA, 2001.
6. [OZD03] Ozdemir, A., Time-Frequency Component Analyzer. Dissertation, Bilkent University, Ankara, Turkey, Sept. 2003.
7. [PAC09] Pace, P., Detecting and Classifying Low Probability of Intercept Radar. Artech House, Norwood, MA, 2009.
8. [PAP95] Papandreou, A., Boudreaux-Bartels, G.F., Kay, S., Detection and Estimation of Generalized Chirps Using Time-Frequency Representations. 1994 Conference Record of the Twenty-Eighth Asilomar Conference on Signals, Systems and Computers, pp. 50-54, 1994.
9. [RAN01] Rangayyan, R., Krishnan, S., Feature Identification in the Time-Frequency Plane by Using the Hough-Radon Transform. Pattern Recognition, Vol. 34, pp. 1147-1158, 2001.
10. [WEI03] Wei, G., Wu, S., Mao, E., Analysis of Multicomponent LFM Signals Using Time-Frequency and The Gray-Scale Inverse Hough Transform. IEEE Workshop on Statistical Signal Processing, pp. 190-193, September 28 – October 1, 2003.
11. [XIA99] Xia, X., Chen, V., A Quantitative SNR Analysis for the Pseudo Wigner-Ville Distribution. IEEE Transactions on Signal Processing, Vol. 47, No. 10, pp. 2891-2894, October, 1999.